

Herwig++ 2.5 Release Note

S. Gieseke¹, D. Grellscheid², K. Hamilton³, A. Papaefstathiou⁴, S. Plätzer⁵, P. Richardson²,
 C. A. Röhr¹, P. Ruzicka⁶, A. Siódmok¹, L. Suter⁷, D. Winn²
 E-mail: herwig@projects.hepforge.org

¹*Institut für Theoretische Physik, Karlsruhe Institute of Technology.*

²*IPPP, Department of Physics, Durham University.*

³*INFN, Sezione di Milano-Bicocca.*

⁴*Cavendish Laboratory, University of Cambridge.*

⁵*Theory Group, DESY Hamburg.*

⁶*Institute of Physics, Academy of Sciences of the Czech Republic.*

⁷*School of Physics and Astronomy, University of Manchester.*

Abstract

A new release of the Monte Carlo program Herwig++ (version 2.5) is now available. This version comes with a number of improvements including: new next-to-leading order matrix elements, including weak boson pair production; a colour reconnection model; diffractive processes; additional models of physics beyond the Standard Model; new leading-order matrix elements for hadron–hadron and lepton–lepton collisions as well as photon-initiated processes.

Contents

1	Introduction	1
1.1	Availability	1
2	POWHEG	2
2.1	Vector Boson Pair Production	2
2.2	$e^+e^- \rightarrow q\bar{q}$	2
2.3	Higgs Decay	3
2.4	Summary	3
3	Colour Reconnection	4
3.1	Review of Cluster Hadronization	4
3.2	Colour Reconnection Algorithm	5
3.3	Effects on Observables	5

4	Diffractive and Photon-Initiated Processes	7
4.1	Photon-Initiated Processes	7
4.2	Diffractive Processes	8
5	BSM Physics	8
5.1	Process Generation	8
5.2	ADD Model	9
5.3	Leptoquarks	10
5.4	NMSSM	10
5.5	Transplanckian Scattering Model	11
5.6	Minor Changes to BSM Models	11
6	New Matrix Elements	11
7	Other Changes	12
8	Summary	17

1 Introduction

The last major public version (2.3) of **Herwig++**, is described in great detail in [1–4]. As we did not produce a release note for version 2.4 we describe all changes since version 2.3 in this release note. The manual will be updated to reflect these changes and this release note is only intended to highlight these new features and the other minor changes made since version 2.3.

Please refer to [1] and the present paper if using version 2.5 of the program.

The main new features of this version are: new next-to-leading order (NLO) matrix elements, including weak boson pair production; a colour reconnection model; diffractive processes; additional models of physics beyond the Standard Model; new leading-order matrix elements for hadron–hadron and lepton–lepton collisions as well as photon-initiated processes.

In addition, the **MC@NLO** [5] program can now generate partonic configurations which can be showered and hadronized using **Herwig++** to produce events with next-to-leading-order accuracy in the **MC@NLO** approach to matching NLO matrix elements and the parton shower.

1.1 Availability

The new program version, together with other useful files and information, can be obtained from the following web site:

<http://projects.hepforge.org/herwig/>

In order to improve our response to user queries, all problems and requests for user support should be reported via the bug tracker on our wiki. Requests for an account to submit tickets and modify the wiki should be sent to herwig@projects.hepforge.org.

Herwig++ is released under the GNU General Public License (GPL) version 2 and the MCnet guidelines for the distribution and usage of event generator software in an academic setting, which are distributed together with the source, and can also be obtained from

<http://www.montecarlonet.org/index.php?p=Publications/Guidelines>

2 POWHEG

The previous version of **Herwig++** included for the first time a number of processes simulated according to the POWHEG NLO parton shower matching scheme [6, 7]. The current release builds on this internal library of NLO-accurate POWHEG simulations, adding doubly resonant W^+W^- , $W^\pm Z^0$ and $Z^0 Z^0$ pair production processes, fermionic Higgs decays and $e^+e^- \rightarrow q\bar{q}$.

This release also sees a major restructuring of the code for the parton shower, in particular the code handling the real emission in the POWHEG scheme, in order to make the implementation of further processes in the POWHEG scheme and other extensions in the future easier.

Previously, the hard and soft matrix element corrections were implemented in a set of dedicated **MECorrection** classes inheriting from the **MECorrectionBase** class. Similarly, the real emission corrections in the POWHEG scheme were implemented in a set of **HardGenerator** classes inheriting from the **HardestEmissionGenerator** base class. While this had some advantages, in particular allowing the corrections to be applied regardless of how the hard processes was generated (for example the corrections could still be used with events read from a LHE file), it led to a significant replication of code between the **HardGenerator** and matrix element classes implementing the \bar{B} function in the POWHEG scheme. We have therefore restructured the code so that both the matrix element corrections and real corrections in the POWHEG scheme are implemented in the matrix element or **Decayer** class implementing the hard scattering or decay process. In addition, the functionality of the separate **PowhegEvolver** has been merged into the base **Evolver** class.

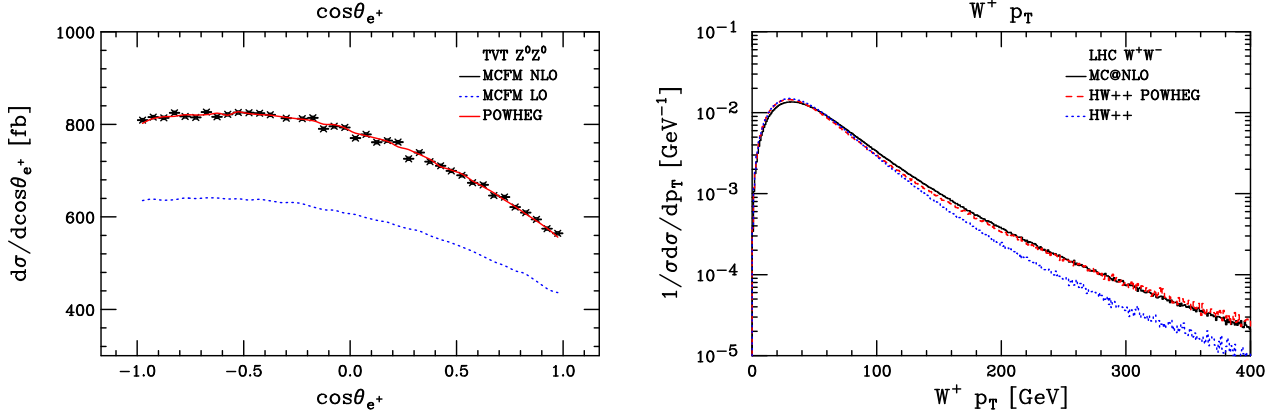
2.1 Vector Boson Pair Production

The simulation of weak boson pair production employs the NLO computations of Refs. [8–10] and its construction has been documented in detail in Ref. [11], together with substantial comparisons to the MCFM and MC@NLO programs [12, 13]. These studies show excellent agreement with MCFM and generally good agreement with MC@NLO. Two examples of these comparisons can be seen in Fig. 1. Note that spin correlations in the vector boson decays are included at tree level for all production modes and decay channels. The simulation of leptonically decaying vector bosons is enhanced, including leading-log photon emission effects resummed according to the YFS formalism [14, 15].

The NLO matrix element class, **MEPP2VVPowheg**, inherits from that of the leading-order matrix element, **MEPP2VV**, thus the selection of particular final states is performed using the **Process** interface. Any one of the five production modes W^+W^- , $W^\pm Z^0$, $Z^0 Z^0$, $W^+ Z^0$, and $W^- Z^0$, can be activated by setting **Process** equal to 1-5 respectively in the input files. Lastly we note that, as with all other **Herwig++** POWHEG simulations, the default renormalization and factorization scale chosen for generating the underlying Born kinematics, *i.e.* the initial $q\bar{q} \rightarrow VV$ configuration, is given by the invariant mass of the colourless final-state system. In generating the hardest emission from this configuration, the renormalization and factorization scales used to evaluate the real cross section are set to the transverse momentum of the emission, as mandated by the POWHEG formalism.

2.2 $e^+e^- \rightarrow q\bar{q}$

The next-to-leading order matrix element for $e^+e^- \rightarrow q\bar{q}$ is implemented, including the masses of the quarks, using the POWHEG scheme in the **MEee2gZ2qqPowheg** class. The virtual corrections were taken from Ref. [16]. The real contribution to both the hardest emission and the \bar{B}



(a) Cosine of the polar angle of a positron produced from a decaying Z^0 boson, in its rest frame, in $Z^0 Z^0$ pair production at the Tevatron ($\sqrt{s} = 1.96$ TeV). The Herwig++ POWHEG prediction is shown in red while the NLO and LO predictions of MCFM appear as black stars and blue dots respectively.

(b) Predictions for the W^+ boson p_T spectrum in $W^+ W^-$ pair production at the LHC, assuming a hadronic centre-of-mass energy of $\sqrt{s} = 14$ TeV. Leading-order Herwig++ results are seen in blue while those of MC@NLO and the Herwig++ POWHEG simulation are visible as black and dashed red lines.

Figure 1: Comparison of Herwig++, MCFM and MC@NLO for di-boson production.

function was calculated using the internal helicity amplitude code. We use the massive dipole scheme of Ref. [17] to subtract the singularities from the real contribution for the calculation of \bar{B} and to separate the singular regions for the generation of the hardest emission.

The results for the cross section for both bottom and top production are in excellent agreement with the analytic results given in the appendix of Ref. [17]. The variation of the cross section for the production of $b\bar{b}$ pairs in e^+e^- collisions with the centre-of-mass energy is shown¹ in Fig. 2(a). The results of this new simulation are in comparable, albeit marginally better, agreement with the data from the LEP experiments, for example the distribution of the thrust shown in Fig. 2(b), than the default Herwig++ approach including a matrix element correction.

2.3 Higgs Decay

There are large QCD corrections to the partial widths for $h^0 \rightarrow q\bar{q}$. As with the simulation of $e^+e^- \rightarrow q\bar{q}$ we use the dipole subtraction scheme of Ref. [17] both to subtract the singularities from the real contribution for the calculation of \bar{B} and to separate the singular regions for the generation of the hardest emission. The internal helicity amplitude code was used to calculate the real emission and the results of Ref. [19] for the virtual contribution. In order to correspond as closely as possible with the masses used in the parton shower, we use the running mass for the coupling of the Higgs boson to the quarks, in order to resum the large corrections, and the pole mass in the kinematics. The resulting simulation is available in the [SMHiggsFermionsPOWHEGDecayer](#) class.

2.4 Summary

For convenience, we give the full complement of NLO-accurate POWHEG simulation classes included in Herwig++:

¹The analytic result is not shown as it is indistinguishable from the Herwig++ result.

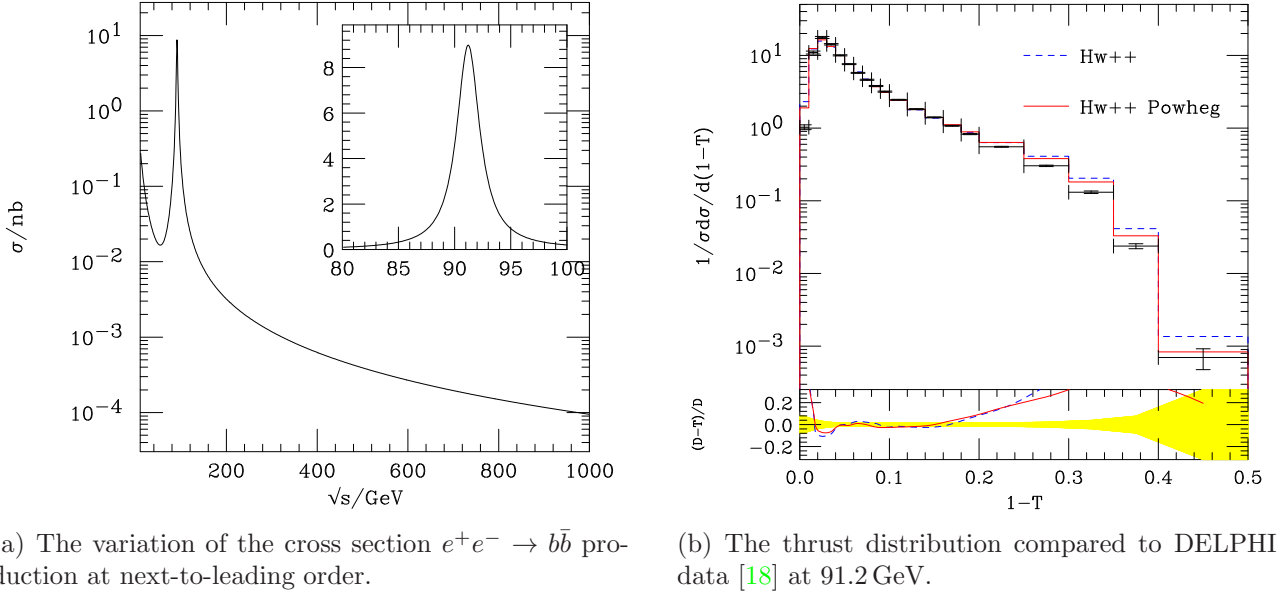


Figure 2: Cross section for $e^+e^- \rightarrow b\bar{b}$ and thrust distribution at LEP.

- the [MEqq2gZ2ffPowheg](#) and [MEqq2W2ffPowheg](#) classes for the production and decay of the γ^*/Z^0 and W^\pm bosons, respectively, in the Drell-Yan process;
- the [MEPP2HiggsPowheg](#) class for the production of the Higgs boson via the gluon-gluon fusion process;
- the [MEPP2ZHPowheg](#) and [MEPP2WHPowheg](#) classes for the production of the Higgs boson in association with the Z^0 and W^\pm bosons, respectively;
- the [MEPP2VVPowheg](#) class for vector boson pair production processes;
- the [MEee2gZ2qqPowheg](#) class for $e^+e^- \rightarrow q\bar{q}$;
- the [SMHiggsFermionsPOWHEGDecayer](#) class for Higgs boson decay into quark-antiquark pairs.

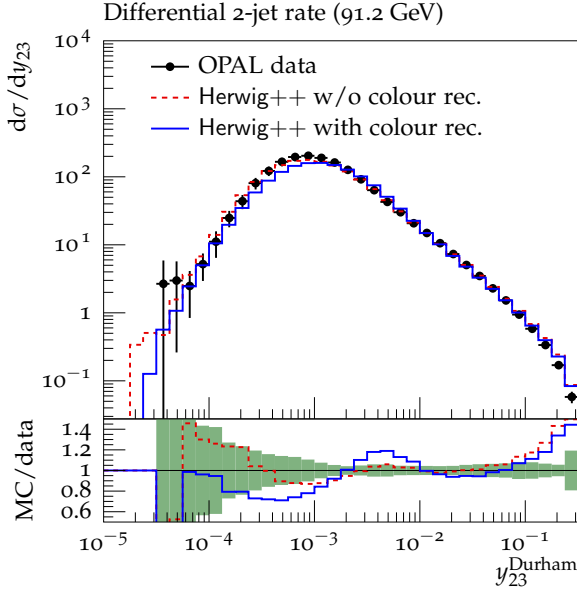
Examples illustrating the use of all of these POWHEG processes can be found in the `LHC-Powheg.in` and `TVT-Powheg.in` example files provided in the release.

3 Colour Reconnection

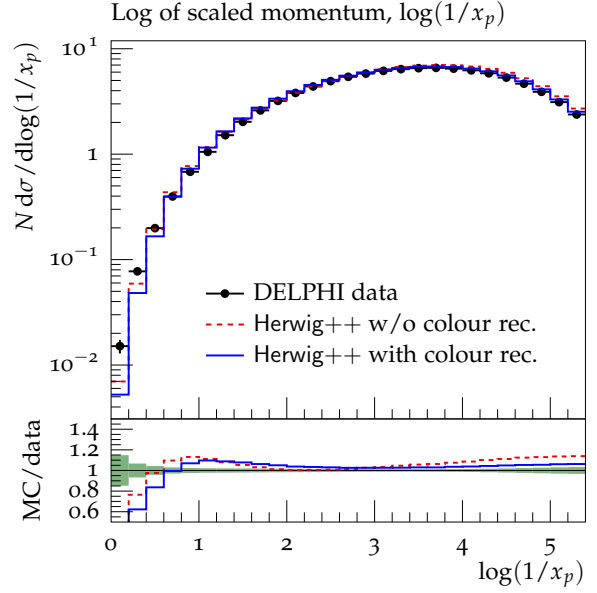
As of this release of `Herwig++`, a model for colour reconnection is included. It is implemented in the [ColourReconnector](#) class. The model can be regarded as an extension of the cluster model [20], which is used for hadronization in `Herwig++`. We would like to stress, however, that this colour reconnection model differs from the one used in (FORTRAN-) `HERWIG` [21], which is based on the spacetime structure of the event as described in Ref. [22].

3.1 Review of Cluster Hadronization

Hadronization in `Herwig++` is based on the pre-confinement property of perturbative QCD [23]. According to that, a parton shower evolving to the cut-off scale Q_0 ends up in a state of



(a) Differential 2-jet rate, data from Ref. [24].



(b) Momentum of charged particles scaled to the beam momentum, data from Ref. [18].

Figure 3: Example distributions comparing an old tune of **Herwig++** without colour reconnections to a new tune including colour reconnections.

colourless parton combinations with finite mass of $\mathcal{O}(Q_0)$. In the cluster hadronization model, these parton combinations – the clusters – are interpreted as highly excited pre-hadronic states. They act as a starting point for the generation of hadrons via cluster decays, which is possibly performed in multiple steps. This hadronization model is described in more detail in Ref. [1].

3.2 Colour Reconnection Algorithm

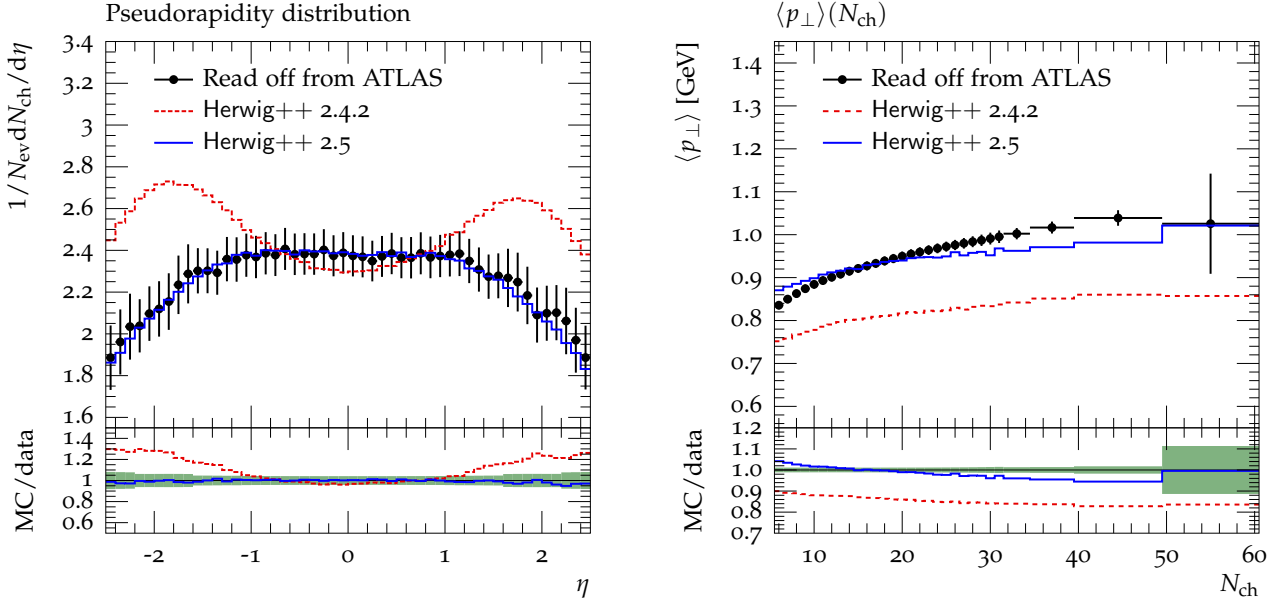
Colour reconnection in the cluster model occurs at the stage where clusters are formed from the parton-shower products. Starting with the clusters that are produced generically by virtue of pre-confinement, the cluster creation procedure is slightly modified. This is done by allowing pairs of clusters to be ‘reconnected’. That means the coloured constituent of cluster A and the anti-coloured constituent of cluster B form a new cluster, as do the remaining two partons.

The following steps are performed for each cluster:

1. loop over all other existing clusters and choose the one where a reconnection of the two clusters would result in the smallest sum of cluster masses;
2. if such a reconnection possibility is found, accept it with probability **ReconnectionProbability**.

3.3 Effects on Observables

A re-tuning of the parton-shower and hadronization-related parameters to LEP data was inevitable since this model for non-perturbative colour reconnection affects hadronization. We find agreement with the LEP data at a similar level to that achieved by the old **Herwig++** tune without colour reconnection. As an example, the 2-jet rate using the Durham jet algo-



(a) Charged-particle multiplicity as a function of pseudorapidity.

(b) Average transverse momentum versus charged-particle multiplicity.

Figure 4: Comparison of **Herwig++** 2.4.2 and **Herwig++** 2.5 to ATLAS minimum-bias distributions at $\sqrt{s} = 0.9$ TeV with $N_{\text{ch}} \geq 6$, $p_{\perp} > 500$ MeV and $|\eta| < 2.5$. The ATLAS data were read off from plots published in Ref. [25].

rithm is shown in Fig. 3(a). A further illustration is given in Fig. 3(b), which shows the scaled momentum of charged particles at LEP.

Since colour reconnection explicitly affects the cluster mass spectrum, the average multiplicity of charged particles changes. This observable was measured to be $\langle N_{\text{ch}} \rangle = 20.92 \pm 0.24$ at LEP for $\sqrt{s} = 91.2$ GeV [18]. With $\langle N_{\text{ch}} \rangle_{\text{Hw++}} = 20.73$ **Herwig++** (with colour reconnection) coincides with this measurement.

Major improvements, however, are achieved in the description of minimum bias events and the underlying event in hadron collisions. In Fig. 4 we show the pseudorapidity distribution of charged particles and their average transverse momentum as function of the charged-particle multiplicity for minimum bias events at $\sqrt{s} = 0.9$ TeV at the LHC. This direct comparison of the current **Herwig++** release to its predecessor shows the progress in modelling minimum-bias events, partially enabled by the presence of non-perturbative colour reconnection.

A second ingredient for the latest developments in the minimum bias and underlying event modelling is a modification of the model for soft interactions in **Herwig++** [26]. The previous model generated additional soft scatters, implemented as soft gluon collisions in di-quark scatterings, in a way that their colour structure is entirely disconnected from the rest of the event. We extend this choice by allowing a colour connection between the soft scatters and the beam remnants. The parameter **colourDisrupt** is the probability of a soft scatter to be disconnected.

Herwig++ is also capable of reproducing minimum-bias data at 7 TeV, as well as underlying-event-related observables for both 0.9 TeV and 7 TeV. Different tunes for each application have to be used, though, since a proper description of all energies with the same set of parameters is not possible with the present model. A more generally applicable model is intended for future **Herwig++** releases. The default parameters in the current release remain those used in the previous version, *i.e.* no colour reconnections are included. The best parameters including

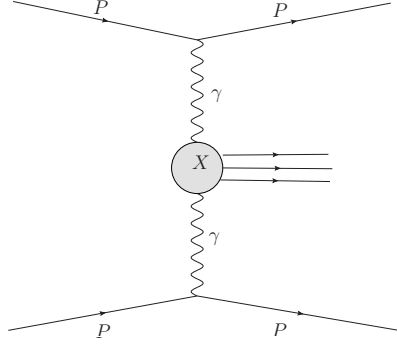


Figure 5: Diagram of a two-photon induced process.

colour reconnections for different processes and energies can be found at

http://projects.hepforge.org/herwig/trac/wiki/MB_UE_tunes

4 Diffractive and Photon-Initiated Processes

Some interesting forward processes in hadron–hadron collisions have been added in this version of **Herwig++**, namely photon-initiated processes and inclusive hard diffractive processes.

4.1 Photon-Initiated Processes

In photon-initiated processes photons are emitted by the incoming protons and their interaction yields a system X which is separated by large rapidity gaps in the forward region from the outgoing scattered protons. The protons remain intact in the interaction and they are only scattered by a small angle. A sketch of the interaction $pp \rightarrow p + \gamma + \gamma + p \rightarrow p \oplus X \oplus p$, where \oplus stands for a rapidity gap, can be seen in Fig. 5. The emission of photons by protons is well described by Quantum Electrodynamics in the framework of Equivalent Photon Approximation [27]. The Photons are almost real (the photon virtuality $Q^2 \sim 0$) and therefore the cross section can be factorized into the photon fluxes and the sub-matrix element. The photon flux is implemented in the **BudnevPDF** class. The photons are generated according to

$$dN = \frac{\alpha}{\pi} \frac{dE_\gamma}{E_\gamma} \frac{dQ^2}{Q^2} \left[\left(1 - \frac{E_\gamma}{E}\right) \left(1 - \frac{Q_{\min}^2}{Q^2}\right) F_E + \frac{E_\gamma^2}{2E^2} F_M \right], \quad (1)$$

where E_γ is the photon energy, E is the energy of proton and Q_{\min}^2 is the minimum virtuality of the photon allowed by the kinematics. The electric and magnetic form factors, F_E and F_M , are given by

$$F_E = (4m_p^2 G_E^2 + Q^2 F_M) / (4m_p^2 + Q^2), \quad (2a)$$

$$G_E^2 = F_M / \mu_p^2 = (1 + Q^2 / Q_0^2)^{-4}, \quad (2b)$$

with the magnetic moment of the proton $\mu_p = 7.78$, the fitted scale $Q_0^2 = 0.71 \text{ GeV}^2$ and the proton mass m_p . An example input file example for LHC settings, **LHC-GammaGamma.in**, is provided in the release.

4.2 Diffractive Processes

In the double pomeron exchange process both protons are left intact by the scattering process and two rapidity gaps occur in forward regions. In single diffractive processes one proton dissociates, while the other is left intact, and a rapidity gap appears on one side of the event. Examples of both processes are shown in Fig. 6. The Ingelman-Schlein model [28] has been implemented to describe those processes. In this model the cross section factorizes into a diffractive distribution function and the cross section of the sub-process, $\sigma = f_D(x, Q^2, x_{\mathbb{P}}, t) \otimes \sigma_{\text{sub}}(x, Q^2)$. The diffractive distribution function can be further decomposed into the pomeron/reggeon flux and distribution functions, respectively,

$$f_D(x, Q^2, x_{\mathbb{P}}, t) = f_{\mathbb{P}/p}(t, x_{\mathbb{P}}) f_{i/\mathbb{P}}(Q^2, x) + \eta_{\mathbb{R}} f_{\mathbb{R}/P}(t, x_{\mathbb{R}}) f_{i/\mathbb{R}}(Q^2, x), \quad (3)$$

where $f_{\mathbb{P}}(t, x_{\mathbb{P}})$ and $f_{\mathbb{R}}(t, x_{\mathbb{R}})$ are pomeron and reggeon fluxes. We use the Regge theory inspired form

$$f_{\mathbb{P}(\mathbb{R})}(t, x_{\mathbb{P}(\mathbb{R})}) = A_{\mathbb{P}(\mathbb{R})} e^{\beta_{\mathbb{P}(\mathbb{R})} t} / x^{2(\alpha_{\mathbb{P}(\mathbb{R})0} - \alpha'_{\mathbb{P}(\mathbb{R})} t) - 1}, \quad (4)$$

where $\alpha_{\mathbb{P}(\mathbb{R})0}$ and $\alpha'_{\mathbb{P}(\mathbb{R})}$ are the pomeron/reggeon intercept and slope, respectively. Both the pomeron and reggeon fluxes are implemented in the `PomeronFlux` class because they differ only in choice of α_0 and α' . The pomeron distribution function $f_{i/\mathbb{P}}(Q^2, x)$ is implemented in the `PomeronPDF` class. `Herwig++` includes the 2006 Fit A, 2006 Fit B and 2007 fits of the pomeron distribution function measured at HERA [29, 30]. The `PomeronPDF` class allows the user to freeze or extrapolate the pomeron distribution functions outside the limits of the experimental fit. In the case of the reggeon distribution function, $f_{i/\mathbb{R}}(Q^2, x)$, an external (pion) parton distribution function from LHAPDF [31] can be used and `Herwig++` provides only the interface class `ReggeonPDF` which mimics a reggeon beam particle and calls an external user-defined PDF. Interfaces to change parameters such as $\alpha_{\mathbb{P}(\mathbb{R})0}$, $\alpha'_{\mathbb{P}(\mathbb{R})}$ and $\eta_{\mathbb{R}}$ are provided. By default they are set to the values determined in the used PDF fit.

We also provide two options for the internal valence structure of the pomeron. The pomeron can be composed of either valence $q\bar{q}$ or valence gluons, the latter of which is the default setting. The reggeon is treated as a $q\bar{q}$ object since using the pion PDF is a usual and consistent approach to describe the reggeon.

The pomeron or reggeon contributions can be simulated either separately or as a mixture. An example of the settings for the LHC can be found in the `LHC-Diffractive.in` input file supplied with the release. It should be noted that the model does not include the gap survival probability factors which need to be taken into account in hadron-hadron collisions.

5 BSM Physics

In addition to including more models of physics beyond the Standard Model (BSM), this release includes a number of other improvements to the simulation of BSM physics in `Herwig++`.

5.1 Process Generation

The inheritance structure of the code for simulating general or resonant $2 \rightarrow 2$ scattering processes has been changed. A new `HardProcessConstructor` base class has been added. The existing code for general $2 \rightarrow 2$ scattering processes has been renamed `TwoToTwoProcessConstructor` and now inherits from the new `HardProcessConstructor` base class, as does the `ResonantProcessConstructor` class for resonant $2 \rightarrow 2$ scattering processes. As

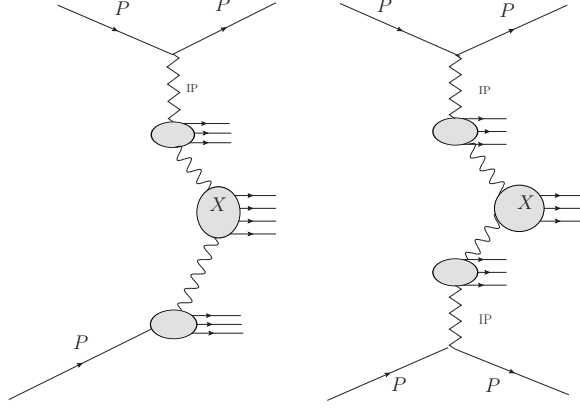


Figure 6: Examples of single diffractive (left) and double pomeron exchange (right) processes.

part of this change, the specific interfaces to the objects needed to simulate $2 \rightarrow 2$ scattering processes have been removed from the `ModelGenerator` class and replaced by a list of `HardProcessConstructors` in order to make adding further types of hard processes easier.

These changes have allowed the generation of hard scattering processes in BSM models to be extended to include some $2 \rightarrow 3$ processes involving neutral Higgs bosons. The production of Higgs bosons in association with an electroweak vector boson, W^\pm and Z^0 , is generated using the `HiggsVectorBosonProcessConstructor` class. The production of a Higgs boson in association with a heavy quark-antiquark pair is calculated using the `QQHiggsProcessConstructor` class. The production of the Higgs boson via the vector boson fusion (VBF) process is simulated using the `HiggsVBFProcessConstructor` class.

In addition, a number of improvements have been made to the hard process selection for $2 \rightarrow 2$ scattering processes in BSM models. The `Processes` interface can be used to select between: `[SingleParticleInclusive]` where at least one of the particles in the list of `Outgoing` particles must be produced, which is the previous behaviour and the new default; the `[TwoParticleInclusive]` option where both the particles produced must be in the list of `Outgoing` particles; and the `[Exclusive]` option where only two particles are allowed in the list of `Outgoing` particles and both of these must be produced. In addition, the `Excluded` interface can be used to forbid specific particles as intermediate particles in the scattering process. Similarly the `ExcludedVertices` interface can be used to forbid specific vertices in the hard scattering processes.

The scale choice in the hard $2 \rightarrow 2$ scattering processes in BSM models can now be changed via the new `ScaleChoice` interface to choose between \hat{s} (default for colour-neutral intermediates) and the transverse mass (default for all other processes).

5.2 ADD Model

In the ADD Model [32–38] gravity propagates in extra spatial dimensions, which have a flat metric. The large size of these extra dimensions leads to a tower of Kaluza-Klein excitations of the graviton. They can either contribute as virtual particles to Standard Model (SM) processes, or be produced leading to missing energy signatures. This model is implemented using the conventions of Ref. [39].

An example input file for the LHC, `LHC-ADD.in`, is provided, and an example of the total cross section for photon or jet production with missing transverse energy is shown in Fig. 7.

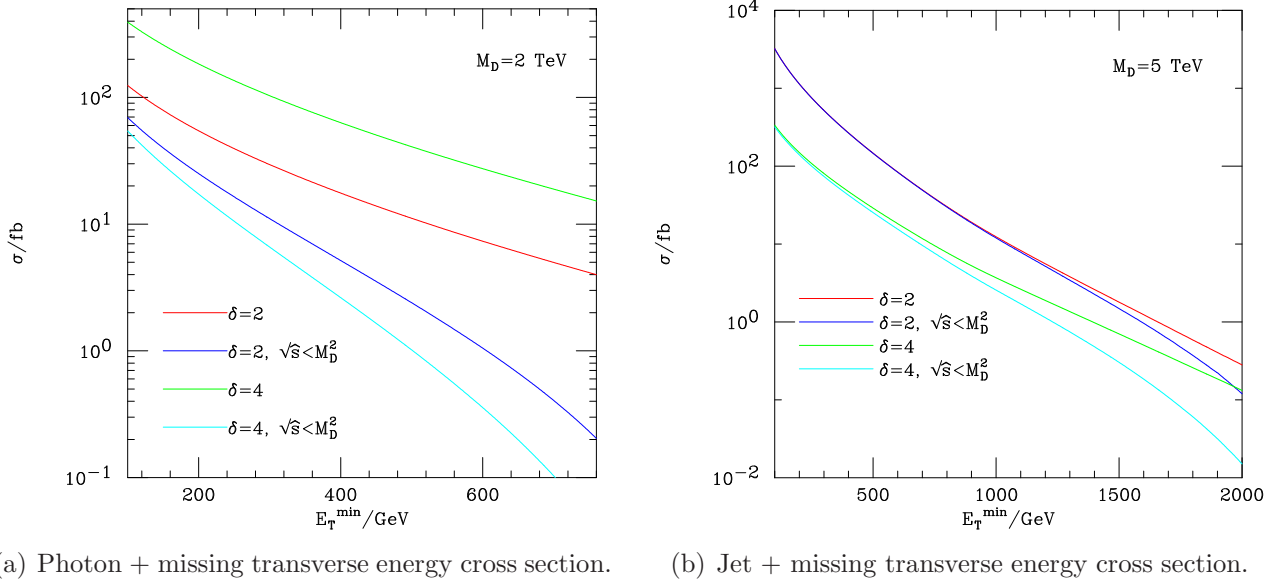


Figure 7: The total photon and jet + missing transverse energy cross section at the LHC. The photons/jets are required to have transverse energy greater than E_T^{\min} . The pseudorapidity of the photons/jets are required to satisfy, $|\eta_\gamma| < 2.5$ and $|\eta_{\text{jet}}| < 3.0$, respectively. The cross section is integrated over either all values of \hat{s} or $\hat{s} < M_D^2$. This figure is based on Figs. 3 and 5 of Ref. [39].

5.3 Leptoquarks

Fermion masses may arise from the mixing of elementary fermions with composite, fermionic resonances of a strong sector [40] responsible for the breaking of the $SU(2)_L \times U(1)_Y$ electroweak symmetry of the SM. It follows that this strongly-coupled sector must also be charged under colour $SU(3)$ and must contain, at the very least, colour-triplet fermionic resonances that can mix with the elementary colour triplets to make the observed quarks. It is reasonable to expect that such a strongly-coupled sector will contain other coloured resonances. These may be bosonic and, depending on their charges, may couple to a quark and a lepton. These leptoquark resonances may be light if they arise as pseudo-Nambu Goldstone bosons and make an ideal target for LHC searches. They will decay exclusively to third-generation fermions due to suppression of the couplings to light fermions.

The present implementation includes non-derivatively coupled leptoquarks, that couple to Standard Model fermions as in Eq. (2.4) of Ref. [41] and single-derivatively coupled leptoquarks such as those in Eq. (2.5) of Ref. [41]. In the case of the derivatively coupled leptoquarks, the simplification that the primed lepton and primed quark couplings are equal has been made.

5.4 NMSSM

The Next-to-Minimal Supersymmetric Standard Model (NMSSM) extends the Minimal Supersymmetric Standard Model (MSSM) with the addition of a singlet Higgs superfield, \hat{S} . This leads to a larger particle content than the MSSM, *i.e.* 3 scalar Higgs bosons, 2 pseudoscalar Higgs bosons and 5 neutralinos. This model has been shown to overcome or reduce many problems associated with the MSSM. For recent reviews of the NMSSM see Refs. [42, 43].

The phenomenologically relevant trilinear interactions of the Higgs bosons with fermions, sfermions, gauginos, gauge bosons, gluons, photons and the other Higgs bosons are included. All the other important interactions are inherited from the implementation of the Minimal Supersymmetric Standard Model. More details are available in Ref. [44].

5.5 Transplanckian Scattering Model

The interaction described by the Transplanckian matrix element is $2 \rightarrow 2$ high-energy gravitational scattering of partons using the eikonal approximation [45]. The approximation is valid in the high-energy, low-angle scattering regime, where the centre-of-mass scattering angle of the incoming parton $\hat{\theta} \rightarrow 0$ or, in terms of Mandelstam variables, $-\hat{t}/\hat{s} \rightarrow 0$. The implementation allows variation of the Planck scale, M_D , as well as the number of extra dimensions, up to a maximum of 6.

5.6 Minor Changes to BSM Models

The `SusyBase` class has been modified so that it can read the SLHA parameter file from the header of a Les Houches event (LHE) file. The name of the LHE file must be given via the `setup` command to the model class instead of the SLHA file.

The vertices for the interactions of gravitinos in SUSY models have been added to allow the decay of the next-to-lightest supersymmetric particles (NLSP) in gauge-mediated SUSY breaking models. In addition, the approach used to calculate Rarita-Schwinger spinors for spin- $\frac{3}{2}$ particles has been changed to improve the numerical stability for very light spin- $\frac{3}{2}$ particles, such as the gravitino.

Similarly, the vertex for the flavour-changing interaction of the stop quark, neutralino and charm quark has been added to allow the simulation of the decay of the lightest stop at parameter points where its mass is lighter than that of the lightest chargino.

In general, `Herwig++` does not include some three- and four-point vertices which do not have any phenomenologically relevant collider signals, for example three- and four-point self couplings of the Higgs boson and the four-point coupling of two vector and two Higgs bosons. Although these interactions are not relevant for the processes we include in the Standard Model, they can be in BSM models, due to the additional particle content. We have therefore extended the implementation of the Standard Model to include the triple Higgs boson self coupling and the coupling of two Higgs bosons to two vector bosons to make implementing these vertices in BSM models simpler. These vertices are also implemented in both the MSSM and NMSSM.

The handling of the colour flows in $2 \rightarrow 2$ hard scatterings has been changed to improve the generality of the code and make future extensions easier. There should be no changes to the results for the currently implemented models. In addition, a number of improvements were made for the colour flows involving colour singlet exchange in the s -channel to allow the simulation of resonant Higgs boson production.

The `Helicity` classes in `ThePEG` have been significantly cleaned up, leading to major simplification of the vertex implementations for all Standard Model and BSM physics models in `Herwig++`. The separate `SpinBase` and `SpinInfo` classes have been merged into the new `SpinInfo` class significantly simplifying the code structure and reducing the number of pointer casts. These changes, which should be transparent to most users, have been made to the helicity amplitude code in order to improve the structure of the code and make future extensions easier.

6 New Matrix Elements

A number of new matrix elements are included in this release:

- the `MEPP2HiggsVBF` for the production of the Higgs boson via electroweak vector boson fusion in hadron-hadron collisions²;

²This matrix element is based on the dominant t -channel contribution to this process.

- the [MEPP2VV](#) class for the production of pairs of electroweak gauge bosons, W^+W^- , $W^\pm Z^0$ and $Z^0 Z^0$ in hadron–hadron collisions;
- the [MEPP2VGamma](#) class for the production of an electroweak gauge boson, W^\pm or Z^0 , in association with a photon;
- the [MEPP2QQHiggs](#) class for the production of the Higgs boson in association with a $t\bar{t}$ or $b\bar{b}$ pair;
- the [MEee2VV](#) class for the production of pairs of electroweak gauge bosons, W^+W^- and $Z^0 Z^0$ in lepton–lepton collisions;
- the [MEGammaGamma2ff](#) class for the production of fermion-antifermion pairs in photon–photon initiated processes;
- the [MEGammaGamma2WW](#) class for the production of W^+W^- pairs in photon–photon initiated processes;
- the [MEGammaP2Jets](#) class for the production of jets in photon–hadron collisions via the partonic processes $q\gamma \rightarrow qg$, $\bar{q}\gamma \rightarrow \bar{q}g$ and $g\gamma \rightarrow q\bar{q}$.

7 Other Changes

A number of changes have been made to the implementation of the [SplittingFunctions](#) in the parton shower module. Previously a splitting function class inheriting [SplittingFunction](#) had to be implemented for each combination of the colours and spins of the interacting particles. This has been changed so that now all the possible colour states of the interacting particles are implemented in the base class while the inheriting classes implement the spin structure only. This makes adding new interactions in BSM models simpler. In addition, the option of deleting specific types of branching in the shower has been added.

A number of other more minor changes have been made. The following changes have been made to improve the physics simulation:

- Soft QED radiation in Z^0 decays is now fully 1-loop by default. As part of this change, the old [WZDecayer](#) class, which handled both W^\pm and Z^0 decays, has been split into separate [WDecayer](#) and [ZDecayer](#) classes handling W^\pm and Z^0 decays, respectively.
- Problems with numerical instabilities in the boosts applied to tau lepton decays have been fixed by postponing the tau decays until after the parton shower. A new interface setting [Excluded](#) in the [DecayHandler](#) class is available to prevent decays in the shower step. By default this is only enabled for tau leptons.
- The default PDF set is now the LO* set of Ref. [46]. In addition, the PDFs used in the shower can now be set separately to those in the hard process using the [ShowerHandler](#) interface of the [ShowerHandler](#) class.
- The shower, hadronization and underlying event parameters were retuned against LEP and Tevatron data respectively.
- The mixing of $B_d^0 - \bar{B}_d^0$ and $B_s^0 - \bar{B}_s^0$ mesons has been added. The oscillation of the mesons is simulated including the CP-violating terms. However, there is no special treatment of those modes where both the meson and its antiparticle decay into the same final state.

- The missing colour structures required for a number of decays in BSM models have been added.
- QED radiation is now enabled in all perturbative Standard Model and BSM decays and all perturbative decays by default, where there are no strongly interacting particles involved in the decay.
- Spin correlations are now switched on by default for all perturbative decays.
- New interfaces to the **AcerDet** [47] and **PGS** [48] fast detector simulations are now available in the **Contrib** directory.
- **FastJet** [49] is now the only supported jet finder code. All analyses have been converted to use **FastJet**.
- Improvements have been made to the momentum reshuffling in Deep Inelastic Scattering.
- The **LesHouchesReader** class has been modified to allow processes that violate baryon number to be read from LHE files.
- A number of changes have been made in the parton shower to allow the violation of baryon number in the hard process. The showering of baryon number violating decays was already supported.
- Code for the simulation of the production of W'^{\pm} bosons using the POWHEG approach is now included in the **Contrib** directory.
- μ^- , ν_μ and ν_e , and their antiparticles, are now available as beam particles. They are all supported in the DIS matrix elements. $\mu^+\mu^-$ collisions are supported in the general matrix element code for BSM models but not yet in the hard-coded matrix elements for lepton-lepton scattering.
- The option of bottom and charm quarks is now supported for heavy quark production in the **MEHeavyQuark** class.
- The polarization of tau leptons can now be forced in the **TauDecayer** class to assist in studies of tau polarization.

A number of technical changes have been made:

- The **Tests** directory has been added. It contains many additional input files to perform more detailed tests of the program than are performed by default during **make check**. These tests use both our own internal analyses and many of the analyses available in **Rivet** [50].
- The \LaTeX output has been updated. After each run, a \LaTeX file is produced that contains the full list of citations. Please include the relevant ones in any publication.
- A number of improvements for OS X systems have been made including fixes for the Snow Leopard release.
- **Makefile-UserModules** now includes the **Herwig++** version number. In addition, the compiler flag **-pedantic** is no longer enabled so that user code using **ROOT** will compile.

- The obsolete `KtJet` and `CLHEP` interfaces have been removed.
- The zero-momentum interacting particle used for bookkeeping in Min-Bias events is now labelled as a pomeron.
- K^0/\bar{K}^0 oscillations into $K_{S,L}^0$ now occur at the production vertex of the kaon to give the correct decay length.
- The default scale choice in POWHEG processes is now the mass of the colour-singlet system.
- A new `ZERO` variable has been introduced, which can be used to set any dimensionful quantity to zero avoiding explicit constructs like `0.0*GeV`.
- A number of improvements have been made to the implementation of three-body decays in BSM models.
- The option of redirecting all output to `stdout` is now supported. The files previously ending in `-UE.out` and `-BSMinfo.out` are now appended to the `log` file. They now also obey the `UseStdout` flag.
- The detection of `FastJet` in the configuration process has been improved.
- The interfaces to `Rivet` and `HepMC` have been moved from `Herwig++` to `ThePEG`.
- The configuration process now looks for `ThePEG` in the location specified by `--prefix`.
- Important configuration information is now listed at the end of the configuration process and in the file `config.thepeg`. Please provide this file in any bug reports.
- The `Exception` specifiers in the definition of the `doinit()` etc. member functions have been removed. This may require the removal of the exception specifier after the function name in some user code.
- The SLHA `EXTPAR` block can now be used to set $\tan\beta$.
- The warning threshold for branching ratios not summing to 1 has been relaxed. It is now a user interface parameter.
- The cross section for inelastic scattering for minimum bias processes is now available in the `-UE.out` files.
- A number of classes have been renamed so that tilde is correctly spelt.
- Some deprecated interfaces in the `MPIHandler` class have been removed.
- The unused doubly heavy baryons have been deleted from the input files.
- A number of minor changes have been made to improve the stability of the phase-space integration in particle decays.
- The handling of the debugging flags has been made more consistent. The user now needs to add, for example, `set LHCGenerator:DebugLevel 1` in the input file or the `-d 1` option on the command line in order for any debugging printout, including printing of events to the log file, to be enabled.

- The handling of the PDG codes for particles has been changed in order to prevent problems on 64-bit systems mapping `unsigned int` to `long`.
- The version of `libtool` has been updated to 2.4. We also use the silent rules available in recent versions of `automake`, reducing the output during the compilation of `Herwig++`.
- The version of `LoopTools` used in `Herwig++` has been updated to 2.6.
- A number of `.icc` files have been removed and the corresponding code moved to either the corresponding `.h` or `.cc` files. Similarly a number of unnecessary `inline` directives and unused header files have been removed.
- The implementation of the `HerwigRun` class has been simplified by using more features of the `EventGenerator` class of `ThePEG`.
- A number of changes have been made to fix warning messages from the Intel compiler.
- The inheritance structure of the `SMHiggsWidthGenerator` has been improved to bring it into line with other `WidthGenerator` classes.
- The option of applying a sequential longitudinal and then transverse boost in the `QTildeReconstructor` in order to conserve energy and momentum, rather than one single boost, has been introduced primarily for use by the `MC@NLO` program.
- The interface to the LHAPDF package [31] is now a separate dynamically loadable module `ThePEGLHAPDF.so` rather than being part of `libThePEG.so`.
- The irrelevant three-body decays are no longer included by default when using the Randall-Sundrum model.
- The `LeptonLeptonRemnant` class has been renamed `UnResolvedRemnant` as it is now used in other applications, for example in photon radiation from protons in hadronic collisions.
- The handling of weighted events in the internal `AnalysisHandler` classes has been improved.
- Various changes have been made to allow `Interpolator` objects to be written to a persistent `ThePEG` stream.
- The obsolete `BSMCascadeAnalysis` has been removed.
- A value of the Fermi constant, G_F , is now available in the `StandardModelBase` class. This allowed the removal of several local values of this parameter.
- The handling of initial-state radiation when the incoming hadron is not along the z -axis has been improved.
- The tolerance parameter used to check momentum conservation in the `BasicConsistency` analysis class can now be changed by the user.
- A new switch has been added to the `ModelGenerator` class so that the branching ratios it calculates in BSM models can be outputted in the SLHA format.

The following bugs have been fixed:

- The example input files for Powheg processes now set the NLO α_S correctly, and are run as part of `make check`.
- A problem that led to the truncated shower not being applied in some cases has been fixed.
- An accidental duplication in the calculation of event shapes was removed, they are now only calculated once per event. Several other minor issues in the event shape calculations have also been fixed.
- An initialization problem in the internal MRST PDFs was fixed.
- The scale in the `Vertex` classes can now be zero where physically possible.
- The `Herwig++` main program now correctly treats the `-N` flag as optional.
- The accuracy of boosts in the z -direction has been improved to fix problems with extremely high p_T partons.
- A bug in the implementation of the PDF weight in initial-state $\bar{q} \rightarrow \bar{q}g$ splittings has been fixed.
- A bug in the $\tilde{\chi}^\pm \tilde{\chi}^0 W^\mp$ and charged Higgs-sfermions vertices has been fixed.
- The longitudinal boost of the centre-of-mass frame in hadronic collisions is correctly accounted for now in the generation of QED radiation.
- Numerical problems have been fixed, which appeared in the rare case that the three-momenta of the decay products in two-body decays are zero in the rest frame of the decay particle.
- The numerical stability in the `RunningMass` and `QTildeReconstructor` classes has been improved.
- The stability of the boosts in the `SOPHY` code for the simulation of QED radiation has been improved.
- A problem with forced splittings in the Remnant was fixed.
- A problem with emissions from antiquarks in the soft matrix element correction in $e^+e^- \rightarrow q\bar{q}$ was fixed. This also required a new tune of the shower and hadronization parameters.
- The matrix element correction for QCD radiation in W^\pm decays, which was not being applied, is now correctly used in W^\pm decays.
- The presence of top quark decay modes in SLHA files is now handled correctly.
- Additional protection against problems due to the shower reconstruction leading to partons with $x > 1$ has been added.
- Changes have been made to allow arbitrary ordering of the outgoing particles in BSM processes.

- Two bugs involving tau decays have been fixed. The wrong masses were used in the [KPiCurrent](#) for the scalar form factors and a mistake in the selection of decay products lead to $\tau^- \rightarrow \pi^0 K^-$ being generated instead of $\tau^- \rightarrow \eta K^-$.
- To avoid crashes, better protection has been introduced for the case where diquarks cannot be formed from the quarks in a baryon-number violating process. In addition, the parents of the baryon-number violating clusters have been changed to avoid problems with the conversion of the events to [HepMC](#).
- A bug in the [QEDRadiationHandler](#) class that resulted in no QED radiation being generated in W^- decays has been fixed.
- A number of minor fixes to the SUSY models have been made.
- A fix for the direction of the incoming particle in the calculation of two-body partial widths in BSM models has been made.
- The [LoopTools](#) cache is now cleared more frequently to reduce the amount of memory used by the program.
- Negative gluino masses are now correctly handled.
- A problem with mixing matrices that are not square has been fixed.
- A problem in the matrix element correction in $e^+e^- \rightarrow t\bar{t}$ events has been fixed.
- The [MEee2gZ2ll](#) has been fixed to only include the photon exchange diagram once rather than twice as previously.
- A problem has been fixed that occurred if the same particle was included in the list of [DecayParticles](#).
- A number of minor problems in the vertices for the UED model have been fixed.
- The missing identical-particle symmetry factor in [MEPP2GammaGamma](#) has been included.
- A floating point problem in the matrix element correction for top decays has been fixed.

8 Summary

[Herwig++ 2.5](#) is the seventh version of the [Herwig++](#) program with a complete simulation of hadron-hadron physics and contains a number of important improvements with respect to the previous version. The program has been extensively tested against a large number of observables from LEP, Tevatron and B factories. All the features needed for realistic studies for hadron-hadron collisions are now present and we look forward to feedback and input from users, especially from the Tevatron and LHC experiments.

Our next major milestone is the release of version 3.0, which will be at least as complete as [HERWIG](#) in all aspects of LHC and linear-collider simulation. Following the release of [Herwig++ 3.0](#), we expect that support for the [FORTRAN](#) program will cease.

Acknowledgements

This work was supported by Science and Technology Facilities Council and the European Union Marie Curie Research Training Network MCnet under contract MRTN-CT-2006-035606. SG, SP, CAR and AS acknowledge support from the Helmholtz Alliance “Physics at the Terascale”. We would like to thank all those who have reported issues with the previous release, in particular B. Allanach, A. Buckley, C. Gwenlan, K. Rolbiecki, and J. Tattersall.

References

- [1] M. Bähr *et. al.*, *Herwig++ Physics and Manual*, *Eur. Phys. J.* **C58** (2008) 639–707, [[arXiv:0803.0883](#)].
- [2] M. Bähr *et. al.* arXiv version (v3) of Ref. [[1](#)], updated on 02/12/2008.
- [3] M. Bähr *et. al.*, *Herwig++ 2.2 Release Note*, [arXiv:0804.3053](#).
- [4] M. Bähr *et. al.*, *Herwig++ 2.3 Release Note*, [arXiv:0812.0529](#).
- [5] S. Frixione, F. Stoeckli, P. Torrielli, and B. R. Webber, *NLO QCD corrections in Herwig++ with MC@NLO*, [arXiv:1010.0568](#).
- [6] P. Nason, *A new method for combining NLO QCD with shower Monte Carlo algorithms*, *JHEP* **11** (2004) 040, [[hep-ph/0409146](#)].
- [7] S. Frixione, P. Nason, and C. Oleari, *Matching NLO QCD computations with Parton Shower simulations: the POWHEG method*, *JHEP* **11** (2007) 070, [[arXiv:0709.2092](#)].
- [8] B. Mele, P. Nason, and G. Ridolfi, *QCD radiative corrections to Z boson pair production in hadronic collisions*, *Nucl. Phys.* **B357** (1991) 409–438.
- [9] S. Frixione, P. Nason, and G. Ridolfi, *Strong corrections to WZ production at hadron colliders*, *Nucl. Phys.* **B383** (1992) 3–44.
- [10] S. Frixione, *A Next-to-leading order calculation of the cross-section for the production of W^+W^- pairs in hadronic collisions*, *Nucl. Phys.* **B410** (1993) 280–324.
- [11] K. Hamilton, *A positive-weight next-to-leading order simulation of weak boson pair production*, *JHEP* **01** (2011) 009, [[arXiv:1009.5391](#)].
- [12] J. M. Campbell and R. K. Ellis, *An update on vector boson pair production at hadron colliders*, *Phys. Rev.* **D60** (1999) 113006, [[hep-ph/9905386](#)].
- [13] S. Frixione and B. R. Webber, *The MC@NLO 3.4 Event Generator*, [arXiv:0812.0770](#).
- [14] D. R. Yennie, S. C. Frautschi, and H. Suura, *The Infrared Divergence Phenomena and High-energy Processes*, *Ann. Phys.* **13** (1961) 379–452.
- [15] K. Hamilton and P. Richardson, *Simulation of QED radiation in particle decays using the YFS formalism*, *JHEP* **07** (2006) 010, [[hep-ph/0603034](#)].
- [16] J. Jersak, E. Laermann, and P. M. Zerwas, *Electroweak Production of Heavy Quarks in e^+e^- Annihilation*, *Phys. Rev.* **D25** (1982) 1218.

- [17] S. Catani, S. Dittmaier, M. H. Seymour, and Z. Trocsanyi, *The Dipole Formalism for Next-to-Leading Order QCD Calculations with Massive Partons*, *Nucl. Phys.* **B627** (2002) 189–265, [[hep-ph/0201036](#)].
- [18] **DELPHI** Collaboration, P. Abreu *et. al.*, *Tuning and test of fragmentation models based on identified particles and precision event shape data*, *Z. Phys.* **C73** (1996) 11–60.
- [19] E. Braaten and J. P. Leveille, *Higgs Boson Decay and the Running Mass*, *Phys. Rev.* **D22** (1980) 715.
- [20] B. R. Webber, *A QCD Model for Jet Fragmentation including Soft Gluon Interference*, *Nucl. Phys.* **B238** (1984) 492.
- [21] G. Marchesini *et. al.*, *HERWIG: A Monte Carlo event generator for simulating hadron emission reactions with interfering gluons. Version 5.1 - April 1991*, *Comput. Phys. Commun.* **67** (1992) 465–508.
- [22] B. Webber, *Color reconnection and Bose-Einstein effects*, *J.Phys.G* **G24** (1998) 287–296, [[hep-ph/9708463](#)].
- [23] D. Amati and G. Veneziano, *Preconfinement as a Property of Perturbative QCD*, *Phys. Lett.* **B83** (1979) 87.
- [24] **JADE** Collaboration, P. Pfeifenschneider *et. al.*, *QCD analyses and determinations of α_S in e^+e^- annihilation at energies between 35 GeV and 189 GeV*, *Eur. Phys. J.* **C17** (2000) 19–51, [[hep-ex/0001055](#)].
- [25] *Charged particle multiplicities in $p p$ interactions at $\sqrt{s} = 0.9$ and 7 TeV in a diffractive limited phase-space measured with the ATLAS detector at the LHC and new PYTHIA6 tune*, Tech. Rep. ATLAS-CONF-2010-031, CERN, Geneva, Jul, 2010.
- [26] M. Bähr, J. M. Butterworth, S. Gieseke, and M. H. Seymour, *Soft interactions in Herwig++*, [arXiv:0905.4671](#). Talk given at Multi-Parton Interaction Workshop, Perugia, Italy, 28–31 Oct. 2008.
- [27] G. V. M. V. M. Budnev, I. F. Ginzburg and V. G. Serbo *Phys. Rept.* **15** (1974) 181.
- [28] G. Ingelman and P. E. Schlein, *Jet Structure in High Mass Diffractive Scattering*, *Phys. Lett.* **B152** (1985) 256.
- [29] A. A. et al., *Measurement and QCD Analysis of the Diffractive Deep-Inelastic Scattering Cross Section at HERA*, *Eur.Phys.J.* **C48** (2006) 715–748, [[0606004](#)].
- [30] A. A. et al., *Dijet Cross Sections and Parton Densities in Diffractive DIS at HERA*, *JHEP* **0710:042** (2007).
- [31] M. R. Whalley, D. Bourilkov, and R. C. Group, *The Les Houches Accord PDFs (LHAPDF) and Lhaglu*, [hep-ph/0508110](#).
- [32] N. Arkani-Hamed, S. Dimopoulos, and G. R. Dvali, *The hierarchy problem and new dimensions at a millimeter*, *Phys. Lett.* **B429** (1998) 263–272, [[hep-ph/9803315](#)].

- [33] N. Arkani-Hamed, S. Dimopoulos, and G. R. Dvali, *Phenomenology, astrophysics and cosmology of theories with sub-millimeter dimensions and TeV scale quantum gravity*, *Phys. Rev.* **D59** (1999) 086004, [[hep-ph/9807344](#)].
- [34] J. D. Lykken, *Weak scale superstrings*, *Phys. Rev.* **D54** (1996) 3693–3697, [[hep-th/9603133](#)].
- [35] E. Witten, *Strong Coupling Expansion Of Calabi-Yau Compactification*, *Nucl. Phys.* **B471** (1996) 135–158, [[hep-th/9602070](#)].
- [36] P. Horava and E. Witten, *Heterotic and type I string dynamics from eleven dimensions*, *Nucl. Phys.* **B460** (1996) 506–524, [[hep-th/9510209](#)].
- [37] P. Horava and E. Witten, *Eleven-Dimensional Supergravity on a Manifold with Boundary*, *Nucl. Phys.* **B475** (1996) 94–114, [[hep-th/9603142](#)].
- [38] I. Antoniadis, *A Possible new dimension at a few TeV*, *Phys. Lett.* **B246** (1990) 377–384.
- [39] G. F. Giudice, R. Rattazzi, and J. D. Wells, *Quantum gravity and extra dimensions at high-energy colliders*, *Nucl. Phys.* **B544** (1999) 3–38, [[hep-ph/9811291](#)].
- [40] D. B. Kaplan, *Flavor at SSC energies: A New mechanism for dynamically generated fermion masses*, *Nucl. Phys.* **B365** (1991) 259–278. Revised version.
- [41] B. Gripaios, A. Papaefstathiou, K. Sakurai, and B. Webber, *Searching for third-generation composite leptoquarks at the LHC*, *JHEP* **1101** (2011) 156, [[arXiv:1010.3962](#)].
- [42] U. Ellwanger, C. Hugonie, and A. M. Teixeira, *The Next-to-Minimal Supersymmetric Standard Model*, *Phys. Rept.* **496** (2010) 1–77, [[arXiv:0910.1785](#)].
- [43] M. Maniatis, *The Next-to-Minimal Supersymmetric extension of the Standard Model reviewed*, *Int. J. Mod. Phys.* **A25** (2010) 3505–3602, [[arXiv:0906.0777](#)].
- [44] P. Richardson and L. Suter, *Simulating the NMSSM with Herwig++*, . in preparation.
- [45] G. F. Giudice, R. Rattazzi, and J. D. Wells, *Transplanckian collisions at the LHC and beyond*, *Nucl. Phys.* **B630** (2002) 293–325, [[hep-ph/0112161](#)].
- [46] A. Sherstnev and R. S. Thorne, *Parton Distributions for LO Generators*, *Eur. Phys. J.* **C55** (2008) 553–575, [[arXiv:0711.2473](#)].
- [47] E. Richter-Was, *AcerDET: A particle level fast simulation and reconstruction package for phenomenological studies on high p_T physics at LHC*, [hep-ph/0207355](#).
- [48] J. Conway *et. al.*, “PGS.” Available from <http://www.physics.ucdavis.edu/conway/research/software/pgs/pgs4-general.htm>.
- [49] M. Cacciari, *FastJet: A Code for fast $k(t)$ clustering, and more*, [hep-ph/0607071](#).
- [50] A. Buckley *et. al.*, *Rivet user manual*, [arXiv:1003.0694](#).